

Using an Intermediate Validation Step to Increase CAE Confidence

Christopher Wolfrom*, Megan Lobdell and Hubert Lobo

*Cornell University, DatapointLabs
Ithaca, New York

Abstract: Simulations contain assumptions and uncertainties that a designer must evaluate to obtain a measure of accuracy. The assumptions of the product design can be differentiated from the ones for the solver and material model through the use of a mid-stage validation. An open loop validation uses a controlled test on a standardized part to compare results from a simulation to the physical experiment. From the validation, confidence in the material model and solver is gained. In this study, the material properties of a polypropylene are tested to characterize for an *ELASTIC *PLASTIC model in ABAQUS. A validation of a quasi-static three-point bending experiment of a parallel ribbed plate is then performed and simulated. A comparison of the strain fields resulting from the complex stress state on the face of the ribs obtained by digital image correlation (DIC) vs. simulation is used to quantify the simulation's fidelity.

Keywords: Abaqus/Explicit, Validation

1. Introduction

Simulating a product before creating a prototype manages performance and production risks, saving time and money. With the increasing use of simulation results for design decision making, it is becoming important to test whether finite element analysis is able to produce results that are similar to those obtained through experimental methods. The usefulness of simulations is limitless, especially with complicated loading conditions on complex geometries. By performing validations with standardized parts containing geometric features that probe simulation accuracy, we can increase the confidence in our engineering designs and reduce the number of prototypes. Conversely, a higher knowledge of how a prototype will perform will increase design effectiveness.

In previous work, Borshoff and Roy (Borshoff, 2014) had built a base case validation workflow for the linear analysis of a “Cornell bike crank” made from aluminum. Starting from a university lab experiment seeking to validate simulation using strain gauges, they applied 3D digital image correlation (DIC) methods to measure surface strain removing uncertainties related to strain measurement. Because DIC allows full surface strain visualization, they were able to visually focus their measurements on areas of significant interest. They also adopted a strict loading scenario using universal testing machines (UTMs) so that the load case could be accurately replicated by the simulation. In subsequent work applied to 3D printed metals, Lobdell (Lobdell, 2015) used simulations to modify the geometry of the original bike cranks to create easily observable deformation locations and to add multi-mode deformations that might better probe the simulation.

The primary impetus of our present work was to see if we could create a physical geometry and deformation scenario protocol for non-linear analysis. Many validations become very complicated or fail because there is too much uncertainty in the ability to simulate the experimental test. For our validation, we selected a geometry that had adequate complexity, could be loaded in a manner that we could reproduce in simulation, while exposing regions where surface strain could be accurately measured. For the material, we chose plastics which are known to have simulation fidelity issues due to material modeling limitations: the commonly used elasto-plastic material model being developed for metals is deficient in its ability to adequately describe the non-linear elastic behavior of plastics with accompanying plasticity (Lobo, 2006).

Our process involved three steps. First, we established the validation subject: an injection-molded polypropylene plate with large parallel fins. An Abaqus model of the subject can be seen in Figure 1. For the validation experiment, we performed a three-point bend test on the plate and recorded the surface strain on the fin using DIC as well as the reaction force on the loading pin. In another physical test, we used a simple tensile test to measure the intrinsic material properties of the polypropylene; this data was used to calibrate the material card in Abaqus. In the final step, a simulation of the validation experiment was performed using Abaqus/Explicit to apply the force used in the validation experiment. Surface strains from the simulation were compared to those obtained from the validation experiment.

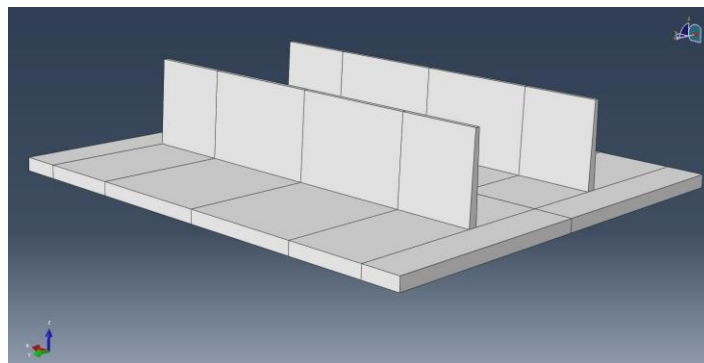


Figure 1: The finned polypropylene plate simulated in Abaqus

2. Methods

2.1 Mechanical

Specially molded plaques made of polypropylene were obtained from Standard Plaque to be used in this study. The plaques contained the finned geometry shown in Figure 1. For the determination of stress-strain data for the material model calibration, ASTM D638 type V tensile bars were cut from flat regions of the plaques using CNC methods. The *Elastic *Plastic material model requires: density, Young's modulus, Poisson's ratio, and uniaxial tensile stress-strain curve decomposed into stress vs. plastic yield strain curve. Tensile testing was performed at a quasi-

static (0.01/s) strain rate on an Instron 8872 universal testing machine (UTM) equipped with contact extensometers. Material model parameters were calculated from tensile testing using Matereality CAE Modeler for Abaqus software. The resultant material cards were imported into Abaqus for analysis; Figure 2 shows the tensile data and material parameters. The material properties and the resulting material model parameters are provided for reference in the Appendix. Properties for the steel used to model the three-point bend fixture are also included there.



Figure 2: Goodness of fit plot for Abaqus elasto-plastic material model created using Matereality

Three-point bend tests were performed using an Instron 8872 universal testing machine (UTM) to provide a test bench for validating the simulation. The specimen rested on two cylindrical supports, each 30 mm long, 10 mm in diameter, separated by a span of 50 mm. They were placed between and perpendicular to the fins, as shown in Figure 3.

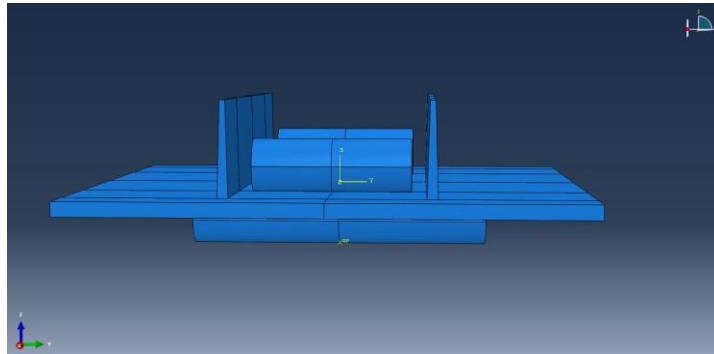


Figure 3: Loading diagram for the finned plate

The loading nose was placed below the plate, perpendicular to the fins, and displaced at a rate of 1 mm/min. This deformed the baseplate, resulting in the fins warping and a tensile strain at the fin tips. The maximum displacement of the loading pin was 19.9 mm with a resulting load of 532.8 N. The maximum load of 952.0 N occurred at a pin displacement of 4.33 mm. A visualization of these results can be seen in Figure 4.

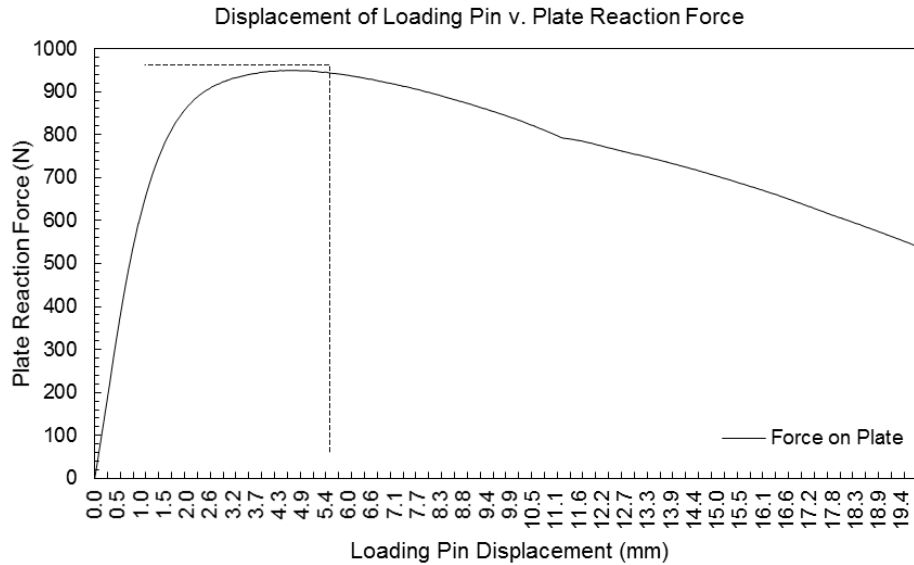


Figure 4: The effects of loading pin displacement on the plate reaction force.

For the experimental measurement of strain, the plate was prepared by applying a speckle pattern on the outside of the fin surface. This region was filmed throughout the experiment with stereo cameras to track the rib displacement. From these images, ARAMIS software calculated the surface strains across the fin (Figure 5).

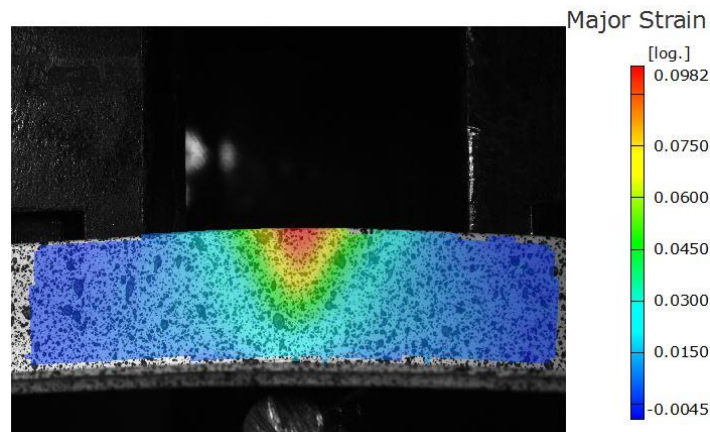


Figure 5: DIC image of major logarithmic strain at 2mm loading pin displacement

2.2 Simulation

Using Abaqus/Explicit, the test was replicated with the goal of creating a simulation that validates the results of the physical testing. In the simulation, the subject was partitioned such that hexagonal elements could be used. These partitions also coincided with reference lines that were created along neutral axes. These axes were useful in constraining the test subject in the simulation. (For reference, the simulation was also set up such that the load was applied in the z-direction, the y-axis is perpendicular to the fins and the x-axis runs parallel to the fins.) In the future, these reference lines could be used to create a quarter model for the sake of preserving computing power and reducing calculation time. The parameters, settings, and constraints of the simulation are summarized in Table 1.

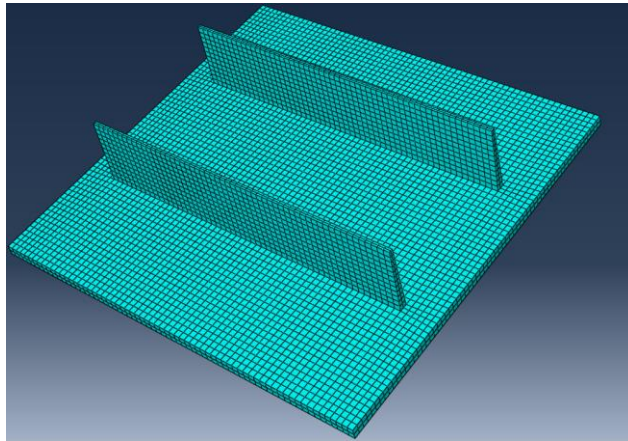


Figure 6: Mesh on plate

Table 1: An overview of the simulation procedure

Mesh Settings			
Mesh Size	Mesh Type	Element Library	Hourglass Setting
1.5 mm	Hex (C3D8R)	Explicit	Enhanced
Position Constraints			
Coincident Point		Edge to Edge	
Loading pin to plate	Support pin to plate	Nose pin to plate	Support pin to plate
Interaction Properties			
Friction Coefficient	0.2	Hard Contact	
Interaction Properties			
Support pin with plate		Loading pin with plate	
Boundary Conditions			
Support pins locked in all degrees of freedom			
Neutral axis reference line parallel to fins constrained to prevent plate movement in y-direction			
Neutral axis reference line perpendicular to fins constrained to prevent plate movement in x-direction			
Loading pin locked in all degrees of freedom except for a 2.5 mm ramped displacement in the z-direction causing a load on the subject.			

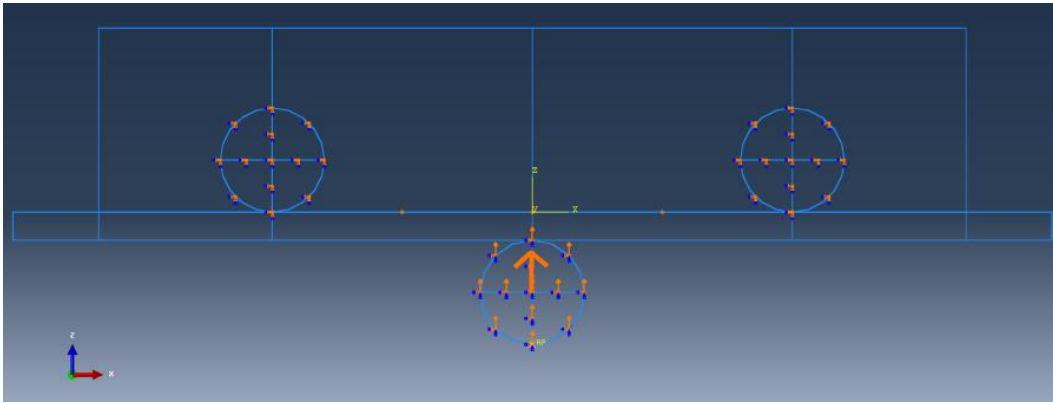


Figure 7: Boundary conditions of the pins on the plate

The mesh was refined to a size of 1.5 mm. This refinement was determined primarily as a result of the fins' response to loading. The region along the fin tip experiences the most thinning and strain; a minimum of two elements are needed. This provides stability for the simulation and better accuracy to calculate strains through the thickness of the fin.

3. Results

Strain field images from the simulation (Figure 8) are presented along with DIC strains from the physical experiment (Figure 9). Both images are set to the same scale for strain so that it is possible to perform a direct comparison of actual strain in the regions of interest. We observe that the local strain fields are similar in shape.

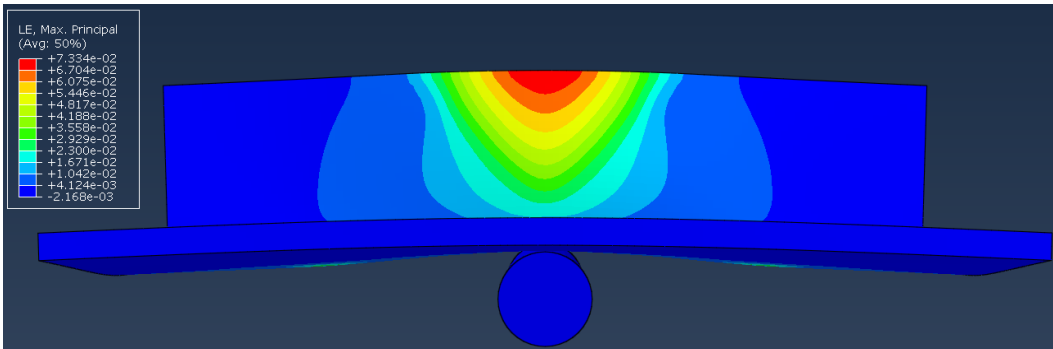


Figure 8: The maximum principal (logarithmic) strain at 2mm loading pin displacement

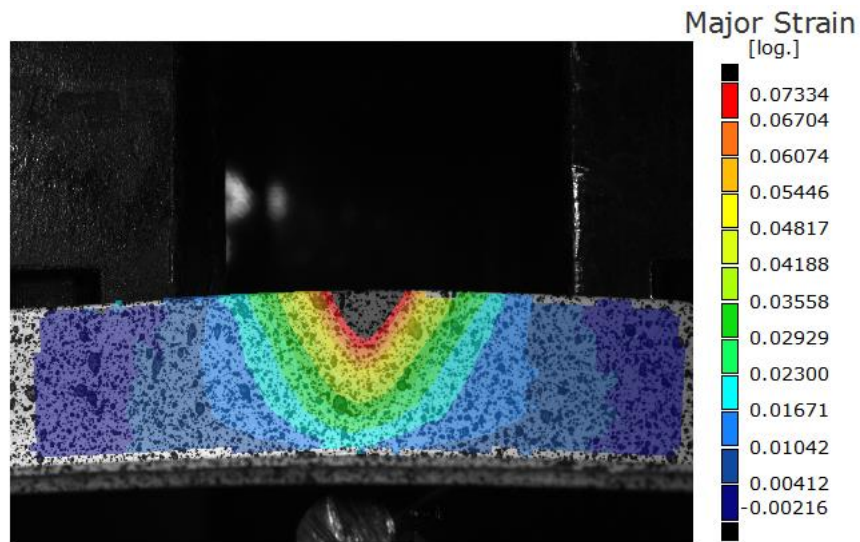


Figure 9: DIC image of major logarithmic strain at 2mm loading pin displacement

At a loading pin displacement of 2 mm, the maximum local strain predicted by the simulation was 7.3% compared to 9.82% measured experimentally by DIC, amounting to a 26% variation. In an effort to understand this variation further, we plotted the maximum strain v. displacement for both the experiment and the simulation (Figure 10). Excellent agreement is observed up to 1.6 mm of displacement after which the simulation begins to diverge dramatically from the experiment.

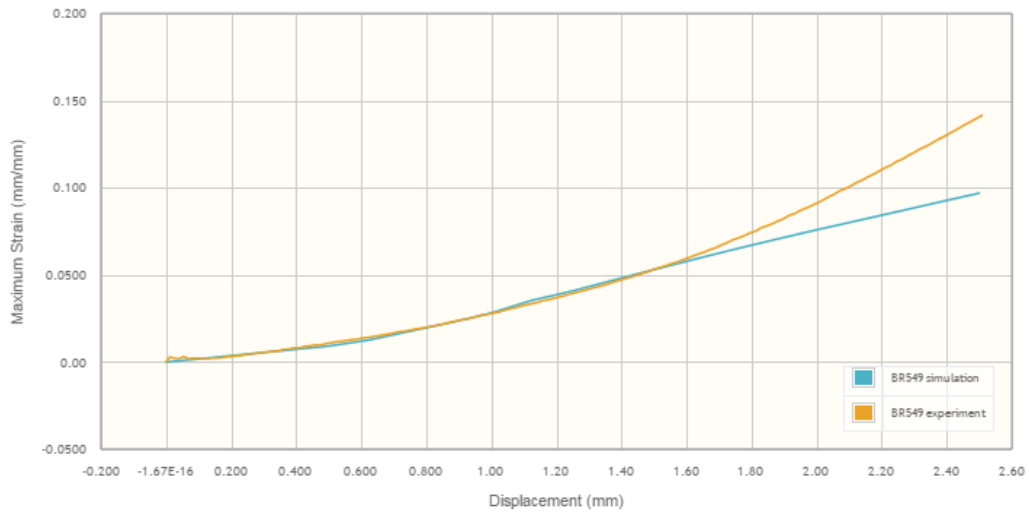


Figure 10: PICSCI comparison plot of maximum strain v. displacement

In contrast, the simulation reaction forces were highly accurate to a displacement of the loading pin of 2 mm (Figure 11). At this displacement, the reaction force on the loading pin was 860.3 N in the experiment and 860.0 N in simulation, with a variation of 0.03%. Beyond this displacement, the simulation begins to diverge from the experiment. One possible reason for these deviations may be that the fins begin to warp into complex and unpredictable geometries with behaviors beyond the capability of the elasto-plastic material model used in this validation. Another possible reason is the mesh refinement used was not sufficient to capture the complex bending shape in the fin.

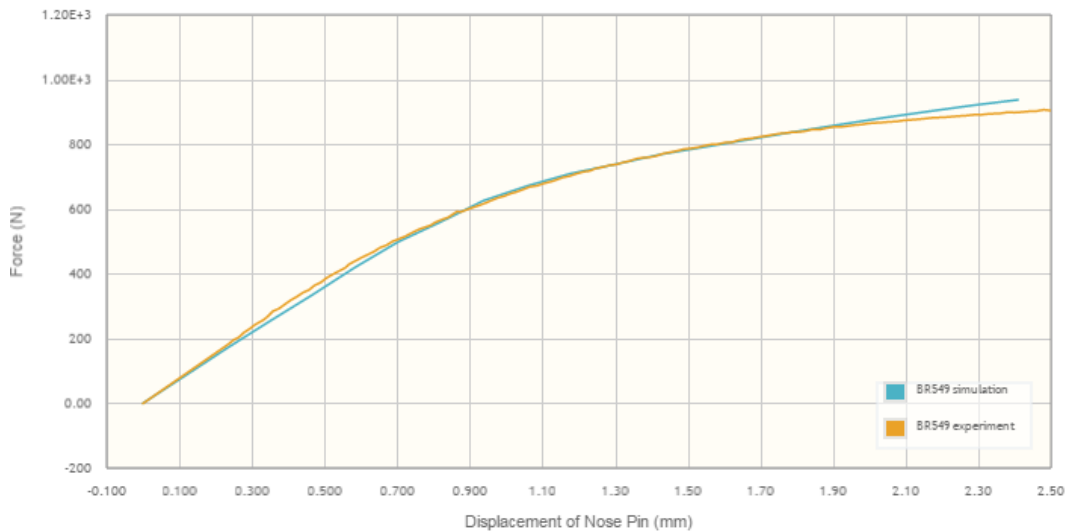


Figure 11: Comparison of force and displacement between simulation and experiment

4. Conclusion

We have performed a simulation validation for a non-linear material using a carefully designed experiment where both the geometry and loading condition can be replicated accurately in the simulation. The Abaqus/Explicit simulation is able to model the elasto-plastic behavior of a ductile plastic with fidelity for moderate strains in a situation where complex modes of deformation are present. The simulation begins to deviate at larger deformations and the model deteriorates as the material model becomes inadequate to describe the actual behavior, a known limitation of using the elasto-plastic material model for polymers (Lobo, 2006). Other factors could also contribute. Further, because of the wide variation in material behavior experienced in plastics, this validation is strictly relevant to the actual material used for the validation. Performing the same validation with other ductile materials can yield different measures of accuracy.

These findings suggest that finite element analysis software has reached a level of sophistication that a simple tensile test provides enough material information to simulate a complex loading scenario on a complex geometry with the potential to eliminate the need to physically test a prototype. We caution against this idea. However, in the current simulation driven product development environment which carries the promise of reduced prototype testing, it can be months before an actual part is created. The knowledge of how much confidence to place in a simulation could be beneficial in such a process allowing the analyst to make good design decisions that can greatly increase the chances of a successful prototype. Validations using standardized parts provide a means to test the assumptions and uncertainties of a simulation against experiment even though the part used in the validation is not the actual part being designed. The choice of contact mechanisms and loading scenarios can be evaluated. In cases where the simulation does not

produce results of adequate accuracy, the same test bench experiment can be used to evaluate alternate solvers, material models or calibration procedures. Because the validation is ‘open-loop’ meaning that it is not one of the experiments used to determine the material parameters in the first place, it is possible to have a much greater confidence in the independence of the result.

5. References

1. J. Borshoff, D. Roy, B. Croop, “The Use of Digital Image Correlation (DIC) and Strain Gauges to Validate Simulation,” NAFEMS USA Regional Conference (2014).
2. M. Lobdell, B. Croop, H. Lobo, “Finite Element Analysis of Additively Manufactured Products,” ANSYS Conference & 33rd CADFEM Users’ Meeting (2015).
3. H. Lobo, J. Hurtado, “Characterization and Modeling of Non-linear Behavior of Plastics,” Abaqus User Conference (2006).

Appendix

Table 2: The Abaqus material model used to simulate the polypropylene

Polypropylene Material Model			
Density [tonne/mm ³]			
1.0034 x 10 ⁻⁹			
Elastic			
Elastic Modulus [MPa]		1572	
Poisson's Ratio		0.33	
Plastic			
Stress [MPa]	Plastic Strain [mm/mm]	Stress [MPa]	Strain [mm/mm]
15.04182	0	30.68552	0.437605
17.46037	0.001956	33.91936	0.549815
19.56054	0.004956	44.34291	0.838261
20.67142	0.00792	58.46458	1.130778
21.44434	0.010993	75.76141	1.389097
22.36164	0.017174	95.1876	1.591274
22.76506	0.022214	108.6908	1.705602
23.08774	0.03784	124.1577	1.810422
23.55031	0.115187	156.7803	1.975266
26.34518	0.258095	192.2232	2.104568
27.4665	0.31128	219.0374	2.196304

Table 3: The Abaqus material model used to simulate the steel loading and support pins

Steel Material Model	
Density [tonne/mm ³]	7.89 x 10 ⁻⁹
Elastic Modulus [MPa]	230,000
Poisson's Ratio	.29